

# A VERY HIGH RESOLUTION HLS USED IN GEOPHYSICS TO RECORD SMALL SIGNALS IN THE FREQUENCY BAND RANGING FROM EARTH FREE OSCILLATIONS UP TO SECULAR TILTS

*Nicolas d'Oreye, MNHN-ECGS, L-7256 Walferdange, Luxembourg (ndo@ecgs.lu)  
Walter Zuern, BFO-Univ. of Karlsruhe, D-77709 Wolfach, Germany*

## 1. INTRODUCTION

Designed initially for Earth tides measurements, this very high sensitivity tiltmeter has showed to be usable for a much broader range of applications and frequency bands. Indeed, the absence of moving parts makes this instrument particularly simple but does not prevent it from measure some very small geophysical signals such as :

- The Earth tides with a very favorable signal-to-noise ratio (e.g. up to 2.000 for the main semi-diurnal  $M_2$  wave which has an amplitude of only 6.3 millisecond of arc<sup>1</sup> in Luxembourg in the 23°N azimuth of the instrument);
- Some very small ter- and quarter-diurnal waves produced by the ocean loading effect from the “shallow-water” tides present in the North Sea distant of 300 km (e.g. the observation of the  $MN_4$  wave in Luxembourg with amplitudes of less than is 0.014 masec);
- The successive passages of seismic surface waves circling the globe after some major earthquakes (e.g. the observation of the Love waves circling 3 times the globe after the Mw 7.9 Denali (Alaska) event on November 3<sup>rd</sup> 2002);
- The free oscillations of the Earth down to the lowest modes excited by some major earthquakes.

The very high stability of the instrument (its drift rate is less than 0.005  $\mu$ rad/month in the underground laboratory of Luxembourg) and its very high resolution and signal-to-noise ratio makes this instrument also useful for other purposes like geotechnical applications or accelerator alignment.

## 2. GENERAL DESCRIPTION OF THE INSTRUMENT

A 43 m long float-less capacitive water-tube tiltmeter named “wth2o” is operating since 1997 in an underground laboratory in Walferdange (Grand Duchy of Luxembourg).

---

<sup>1</sup> 1 masec = 4.848 nrad

It is composed of two aluminum vessels (inner diameter of 20cm) interconnected with two polyethylene tubes (see Figure 1). One has a 2.04cm inner diameter and is filled with distilled water, while the other has a 1.5cm inner diameter and is used for the air pressure balancing. The tubes lie horizontally on a small levee made of gypsum dust that has been built to overcome the gentle slope of the gallery's floor. The horizontality has been checked by a laser technique and the tubes are covered by dust for additional thermal insulation.

The aluminum end vessels, as well as every metallic part of the apparatus, are coated with a mixture of nickel and Teflon [Kanigen® and NIPTEF® methods provided by KANIGEN WORKS BENELUX]. This prevents the corrosion of aluminum (highly chemically reactive) and avoids liquid sticking to the metal.

A 2cm thick layer of MetylSyloxane oil covers the free surface of the water in each end vessel. This prevents water evaporation and does not chemically react with the different parts of the instrument (water, nickel-Teflon, Nylon, O-ring). It does not mix with water and it is a stable dielectric. Very low viscosity oil ( $2.185 \cdot 10^{-3}$  Poiseuille @ 20°C) has been selected to avoid hindering the water displacement [UNISILIKON TK 002/20 from Klüber Lubrication]. Its low surface tension reduces the menisci at the contact line with the vessels walls. Pots are hermetically sealed and connected to each other from their top center for the air pressure balance, and from their bottom center for the liquid level equilibration.

A calibration device is installed at the middle of the instrument. It is made of a vertical tube flanked by two ball valves. This device was also used for filling the instrument. In normal recording conditions, that tube is sealed by means of a thick rubber cork pierced by two high-precision syringes. One of these syringes is mounted into a precision volume dispenser that allows pouring up to 50 equal fractions of the contents (i.e. 2µl in the present case).

A capacitive sensor records the vertical liquid displacement in each head. The lower electrode is actually the bottom of the vessel (cold point of capacitor) while the upper electrode is a 16cm circular aluminum electrode immersed in the oil (hot point). It is held in place at a distance  $H = 12\text{mm}$  from the bottom of the vessel by an 8cm wide Nylon cylinder. The system is equivalent to two capacitors mounted in series: one having the oil as a dielectric and the other filled with the water. The thickness  $d$  of the oil layer below the electrode is about 0.8mm. The theoretical capacitance is hence given by  $C = [\epsilon_o \epsilon_h \epsilon_w A_e f_w f_h] / [\epsilon_w d f_w + \epsilon_h d_w f_h]$ , where  $\epsilon_o$  is the dielectric constant of vacuum,  $\epsilon_w$  and  $\epsilon_h$  are the dielectric constants of the water and the oil respectively,  $d_w$  and  $d$  are the thickness of the water and oil layers between the electrodes,  $A_e$  is the surface of the upper electrode and  $f_w$  and  $f_h$  are empirical factors taking into account the side effects in the circular planar capacitors [1]. The advantage of immersing the capacitor plate into the oil is to reduce the effects on the measurements of oil migration along the vessel's walls, and to reduce the noise.

The electronics used to record the capacitance variations are made of simple R-C oscillators (or "relaxation oscillators"). These electronics are designed with only two electronic amplifiers and few resistors and capacitors [2]. The theoretical frequency output is in our case  $F_{theor} = (2 R C 0.694)^{-1}$ , where  $R$  is a high stability resistor with a drift of less than 5 ppm/yr, and  $C$  is the water-tube capacitance.

The data acquisition system [3] records the frequency of each head simultaneously (of the order of 40 to 50kHz) with a 0.002Hz resolution. The absolute time synchronization is better than 0.01s thanks to the use of a time signal radioed from Frankfurt (DCF). The sampling rate is 1s.

Given the length of the apparatus, the measure of the vertical displacement of the water-oil interfaces (WOI) can easily be transformed into tilt.

The overall instrument is installed in an underground geophysical laboratory hosted in an old 100m deep gypsum mine in Walferdange [4]. The air temperature stability is better than  $0.02^{\circ}\text{C}/\text{yr}$  and  $0.003^{\circ}\text{C}/\text{day}$ . At such a depth these variations correspond to atmospheric adiabatic air pressure effects and hence are uniform all along the instrument.

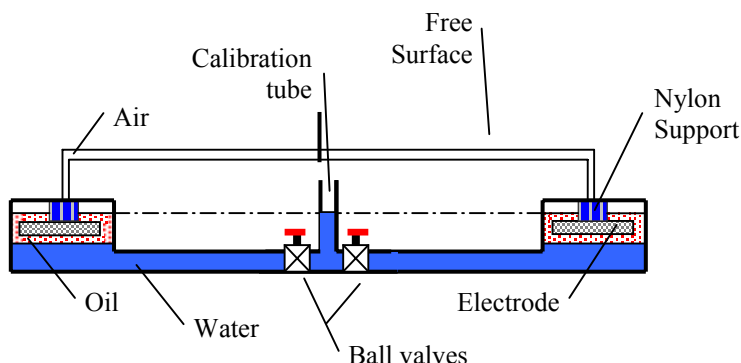


**Figure 1:** Schematic diagram of the “wth2o” float-less water-tube tiltmeter.

### 3. PERFORMANCES

#### 3.1. The resolution

Since the resolution cannot be given as a single value (it depends on the duration of the record, the frequency band and the type of signal – transient or periodic –), one can only state that for a given frequency band, the resolution of the “wth2o” is better than the observed noise level. Table 1 summarizes the observed values of the noise in the corresponding bands. The resolution of the acquisition system is  $0.15 \mu\text{sec}$  (i.e.  $0.0007 \text{ nrad}$ )<sup>2</sup>.

**Table 1:** Observed noise level vs. frequency bands. The resolution of the “wth2o” tiltmeter is better than the noise level in the corresponding frequency bands.

Period [h]	Frequency [mHz]	Band Width [mHz]	Noise level	
			[ $\mu\text{sec}$ ]	[nrad]
24	0.012	0.008 – 0.014	6.2	0.030
12	0.023	0.020 – 0.025	3.3	0.016
8	0.035	0.032 – 0.036	1.4	0.007
6	0.046	0.044 – 0.046	0.9	0.004
1/60	16.7	5.0 – 20.0	1	0.005

#### 3.2. The noise

The noise level of the present instrument (installed in its present location) can be estimated thanks to the Power Spectral Density (PSD) defined as follow [5]:

<sup>2</sup> Note that an angle of  $1 \mu\text{sec}$  (or  $0.005 \text{ nrad}$ ) is the angle supported by an arc of only 5 microns over a distance of 1.000 km.

$$I_N^*(\omega_p) \equiv |\xi_{X'}(\omega_p)|^2 \quad \text{with} \quad \xi_{X'}(\omega_p) = \frac{1}{\sqrt{2\pi N}} \sum_{t=1}^N X'_t e^{-i\omega_p t}, \quad p = 0, 1, \dots, \frac{N}{2} \quad (1)$$

$$X'_t \equiv X_t - \bar{X} \quad \text{and} \quad \bar{X} \equiv \text{avg}\{X_t\},$$

and where  $X_1, \dots, X_N$  are the  $N$  observations. To avoid leakage in the spectrum, one has previously multiplied the  $N$  data by a Hanning window (of parameters  $h_1, \dots, h_N$ ). In addition, to conserve the power, the  $n^{\text{th}}$  measure is multiplied by

$$H_{\text{han}} = (1/N) \sum_{n=1}^N h_n^2 \quad (2)$$

Finally, to take into account the contribution of the power at negative frequencies, the spectrum is multiplied by two. This allows us to compare the PSD with the reference inclinometric low tilt noise model from Agnew[1986] [6].

It can be seen in Figure 2 that the present water-tube exhibits a very low noise up to the long-period seismic band.

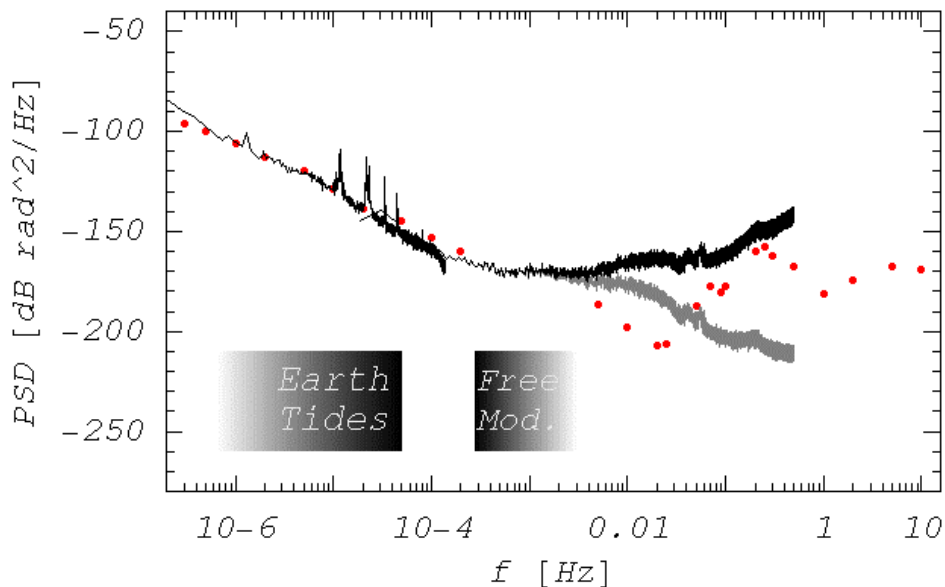


**Figure 2:** Comparison of the Power Spectral Density of the 6 years long “wth2o” record in Walferdange (with and without the instrumental response correction - black and gray curve respectively) and the low tilt noise reference model from Agnew [1986] (red dots). Shaded rectangles pinpoint the frequencies ranges of the Earth tides and the Earth free modes.

### 3.3. The stability

In the environmental conditions of the gypsum mine where it is currently installed (at 100m under ground level), the instrument shows a very low linear drift rate. During the two first years however, the drift reached  $\sim 0.17 \mu\text{rad}/\text{month}$  because of a Water-Oil interface problem. During the 3 next years the drift was still  $\sim 0.05 \mu\text{rad}/\text{month}$ . It has been finally decreased to  $< 0.004 \mu\text{radian}/\text{month}$  thanks to some changes in the electronics (see Figure 3).

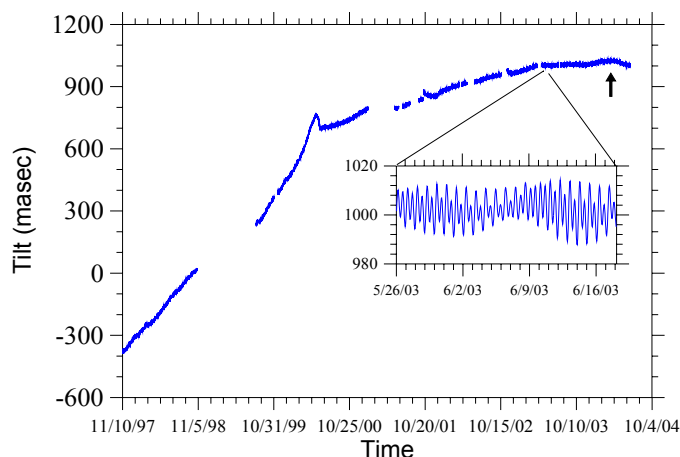


**Figure 3:** Seven years of tilt record with the “wth2o” (from November 1997 to June 2004). The apparent thickness of the curve is due to the Earth tide oscillations as shown in the close-up. The drift decreased respectively after 2 and 5 years to reach a final value of less than  $0.004 \mu\text{rad}/\text{month}$ , which is (one of) the lowest drift rate reported in the literature. The six months long drift (bulge at the black arrow) is due the visit of about 500 people over 10 days.

#### 4. EXAMPLES OF OBSERVATIONS

On November 3<sup>rd</sup> 2002, a major earthquake occurred in the Denali (Alaska). That event allowed us to record the successive passages of the Love seismic surface waves circling 3 times the globe (Figure 4). After the earthquake, seismic waves propagated in, and at the surface of the Earth. The first arrival of the Love surface waves (named G1) occurred while the waves have traveled along the minor (shorter) great circle. The second arrival (G2) appears later and corresponds to the Love waves that have traveled in the mean time trough the major arc path, on the opposite side of the Earth. Both waves packets continued to circle the globe in opposite directions (taking about 3 hours to accomplish a full revolution) and every successive passage are numbered G3, G4 etc... Odd numbers correspond to waves leaving the source in the minor arc directions while even numbered waves are circling the globe in the major arc direction.

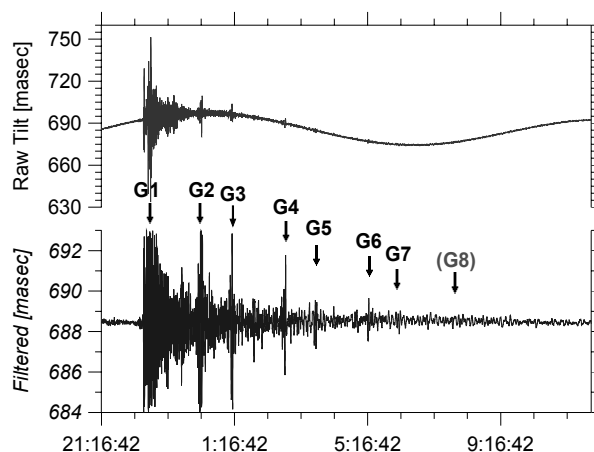


**Figure 4:** Record of the successive passages of the Love surface waves (up to G7 and maybe G8) circling 3 times the globe after the Denali earthquake on November 3<sup>rd</sup> 2002 (Mw 7.9). The upper curve shows the raw tilt data. The lower curve (clipped) shows the same data where the Earth tide signal has been filtered out.

After the same event, thanks to the very low noise level and the high resolution of the instrument up to the long-period seismic band, it was also possible to record the rarely observed gravest toroidal ( ${}_nT_1$ ) and spheroidal ( ${}_nS_1$ ) modes of the Earth free Oscillations (Figure 5).

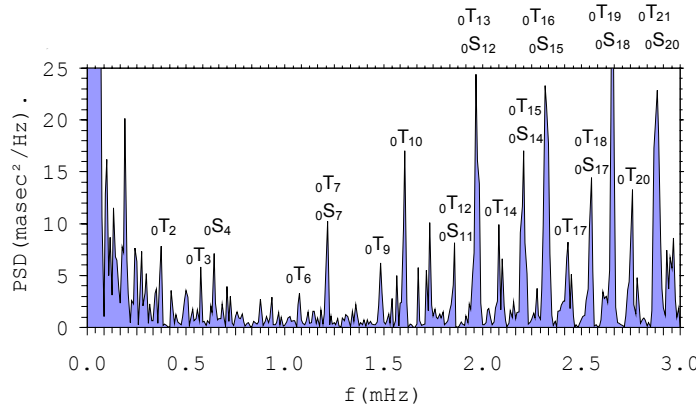


**Figure 5:** Power spectrum of the Denali earthquake recorded by the “wth2o” in Walferdange. Clear spikes show up at the frequencies of the lowest toroidal ( ${}_nT_1$ ) and spheroidal ( ${}_nS_1$ ) Earth free modes. Some of these modes have never been clearly observed in horizontal component.

## 5. FREQUENCY RESPONSE

The frequency response can be deduced from the Laplace transform of the equation of motion (EOM) as long as the EOM is linear and the system is time invariant [7]. A simple pots-and-tube system usually satisfies these conditions<sup>3</sup> and therefore the EOM can easily be calculated [8]:

$$m_0 \ddot{y} + 2\beta\omega_0 m_0 \dot{y} + m_0 \omega_0^2 y = -\frac{3am_0}{4A} \ddot{X} - m_0 \omega_0^2 \frac{l_0 \theta}{2} - M l_0 \ddot{\theta}, \quad (3)$$

where  $y$  is the vertical water displacement in the pot,  $a$  and  $A$  are the cross section of the tube and pots respectively,  $M$  is the mass of liquid present in each pot,  $\theta$  and  $X$  are the angular and lateral displacements of the apparatus, and  $l_0$  is the length of the instrument. Dots indicate the spatial derivative.  $m_0$ ,  $\beta$  and  $\omega_0$ , respectively, are the mass of an equivalent harmonic oscillator, its damping factor and its natural frequency. They are defined here as:  $m_0 = (4mA^2)/(3a^2)$ ,  $\omega_0 = [(3ag)/(2Al_0)]^{1/2}$ , and  $\beta = (3\pi\mu)/(\rho a \omega_0)$ , where  $m$  is the mass of liquid in the tube ( $\rho a l_0$ ),  $g$  is the gravity,  $\rho$  and  $\mu$  are the fluid’s density and dynamic viscosity.

However, taking into account the additional damping due to the oil flow below the capacitors plates renders the EOM non-linear. Indeed, that contribution to the damping will depend first on the vertical displacement  $y$  of the WOI, and secondly on the radial velocity of the liquid at that interface (defined as the time derivative of the radial distance  $r_e$  from the center of the pot), which itself depends also on  $y$ . Moreover, the EOM of such a system cannot be

<sup>3</sup> As long as  $(3Ma^2)/(2mA^2)$  is negligible with respect to unity as it can be seen from the computation of the kinematics’ energy of the liquid in the end vessels.

completely solved analytically because we do not know the radial fluid velocity at the WOI. However, one can compute two extreme solutions: one supposing the velocity to be zero, and the other supposing it to be equivalent to the one that a layer of a single liquid trapped between the electrodes would have at the same distance  $d$  from the upper electrode. For this, we introduce the parameters  $\alpha_+$  and  $\alpha_-$  (the subscripts  $+$  or  $-$  distinguish the vessels where the liquid rises or falls) which take the values  $0 \leq \alpha_+ \leq [3A(d-y)(H-d+y)/(H^3\pi)]$  or  $0 \leq \alpha_- \leq [-3A(d+y)(H-d+y)/(H^3\pi)]$ , respectively. The complete EOM becomes [9]:

$$\begin{aligned}
m_0\ddot{y} + 2\beta\omega_0 m_0\dot{y} - \frac{2\mu_h \ln\left(\frac{r_0}{R_e}\right) \left(3A^2 + 2\pi(d-y)\alpha_+ (-3A + 2\pi(d-y)\alpha_+)\right)}{\pi(d-y)^3} \dot{y} \\
- \frac{2\mu_h \ln\left(\frac{r_0}{R_e}\right) \left(3A^2 + 2\pi(d+y)\alpha_- (-3A + 2\pi(d+y)\alpha_-)\right)}{\pi(d+y)^3} \dot{y} + m_0\omega_0^2 y \\
= -\frac{3am_0}{4A} \ddot{X} - m_0\omega_0^2 \frac{l_0\theta}{2} - Ml_0\ddot{\theta}, \tag{4}
\end{aligned}$$

where  $r_0$  and  $R_e$  are the radius of the water-tube and the electrode<sup>4</sup>, and  $\mu_h$  is the dynamic viscosity of the oil.

One can show that, for an instrument with the characteristics of our prototype, and even for WOI displacements of much larger amplitude than those for which the instrument was supposed to face, these extreme solutions (with  $\alpha_+$  and  $\alpha_-$  null or maximum) do not lead to significantly different numerical solutions. In addition, numerical solutions of the EOM with or without taking into account the vertical displacement of the WOI in the expression of the damping due to the oil flow, do again not lead to significant differences. Hence one can use an approximate EOM for a system where the damping does not take into account either the vertical or the radial displacement of the WOI. Under such conditions, the EOM remains linear:

$$m_0\ddot{y} + 2\beta_L\omega_0 m_0\dot{y} + m_0\omega_0^2 y = -\frac{3am_0}{4A} \ddot{X} - m_0\omega_0^2 \frac{l_0\theta}{2} - Ml_0\ddot{\theta}, \tag{5}$$

$$\text{where } \beta_L = \beta + \frac{-6A^2\mu_h \ln\left(\frac{r_0}{R_e}\right)}{\pi d^3 \omega_0 m_0} \tag{6}$$

Since the system is linear, one can separate the EOM's Laplace transform into two distinct transfer functions:  $G_{tilt}(s)$  for the tilt, and  $G_{disp}(s)$  for the horizontal displacement. In addition, since in our case  $(2M/m_0\omega_0^2) \ll 1$ , one can see that the contribution of the angular acceleration is negligible. The theoretical transfer functions are then given by:

<sup>4</sup> Since our model of damping due to oil flow below the capacitor's upper plate assumes a radial oil flow, we were facing an uncertainty at the center. To solve this, we have arbitrary set to  $r_0$  the radius of a central zone that is ignored. That is why the radius of the water-tube appears in the logarithm. Comparison of model and observations showed that this choice is fairly well adapted to our prototype.

$$G_{\text{tilt}}(s) = \frac{-1}{1 + \frac{2\beta_L}{\omega_0}s + \frac{s^2}{\omega_0^2}} \quad \text{and} \quad G_{\text{disp}}(s) = \frac{-3a}{4A\omega_0^2} \frac{s^2}{1 + \frac{2\beta_L}{\omega_0}s + \frac{s^2}{\omega_0^2}} \quad (7)$$

These transfer functions are used to plot the theoretical Bode plots of the frequency responses (see Figure 6).

To obtain the transfer function experimentally, step response experiments were conducted. A known volume of water (from 100 $\mu$ l to 1ml depending on experiments) was transferred from one head to the other with the help of a syringe at the central calibration tube and an appropriate succession of valve openings and closures. After stabilization, the last valve was opened and the liquid levels equilibrated. Such a signal can be considered as an input of a Heavyside shape. The transfer function is then the FFT of the time derivative of the output signal [10] (recorded here at a one second sampling interval).

Comparing measured and theoretical tilt transfer function shows a good agreement between models and observations up to the cut-off frequency: the agreement is better than 2% in amplitude and 1 degree for the phases.

The remaining discrepancies can be attributed to noise during experiments and small (unavoidable) approximations in the models.

The model used to compute the analytical tilt and acceleration (displacement) transfer functions for this instrument and its sensors (Figure 6) can be used to calculate the best geometrical characteristics for the construction of a new prototype having to respond to specific requirements of a new application in geophysics or geotechnics.

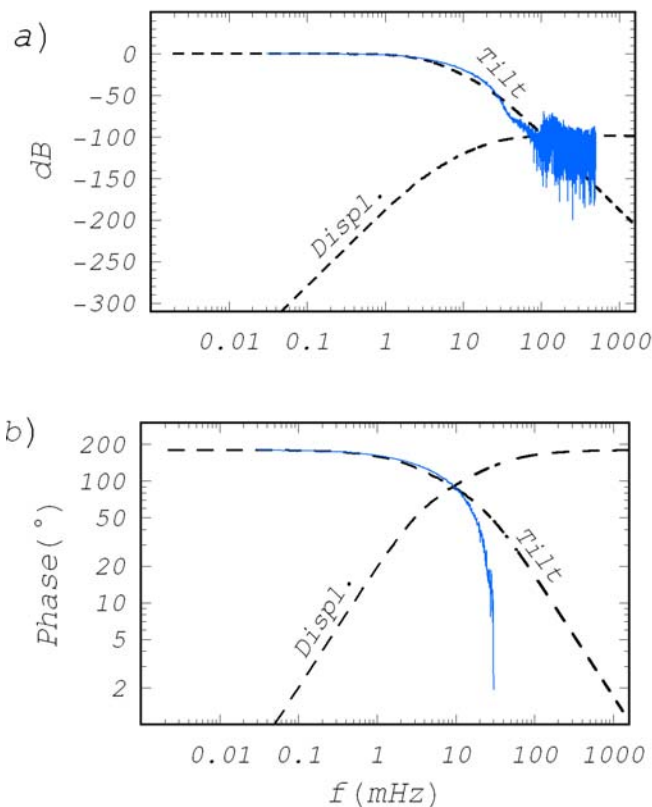


**Figure 6:** Amplitude (a) and phase (b) of the theoretical transfer function for tilt and horizontal displacement (dashed lines) and measured step response for tilt (solid blue lines).

## 6. POSSIBLE LIMITATION OF THE HLS: THE MENISCUS EFFECTS

The way the liquids wet the walls of the instrument (the meniscus effect) can be a limitation for the use of HLS at very high resolution. This is a rather complicate phenomenon (at microscopic and macroscopic level) driven by the physico-chemical properties of the fluids and solids put together.

When the interface between two fluids comes in contact with a solid, the interface at the contact line makes an angle  $\Theta_0$  with the solid surface. This contact angle is a property of the two fluids and the solid. In practice though, if the interface moves, that contact angle can take any value comprise between two extremes values: the advancing and receding angles. The amount of liquid “trapped” in that meniscus can hence vary, which in turn induces a displacement of the liquid interface. For instance, when the fluid level rises in one head (see Figure 7 left), the amount of liquid trapped in the meniscus along the solid wall  $v_0$  will decrease of a small amount  $\delta v_{up}$ . (Similar reasoning applies when the liquid falls (see Figure 7 right): the volume increases of  $\delta v_{down}$ ).

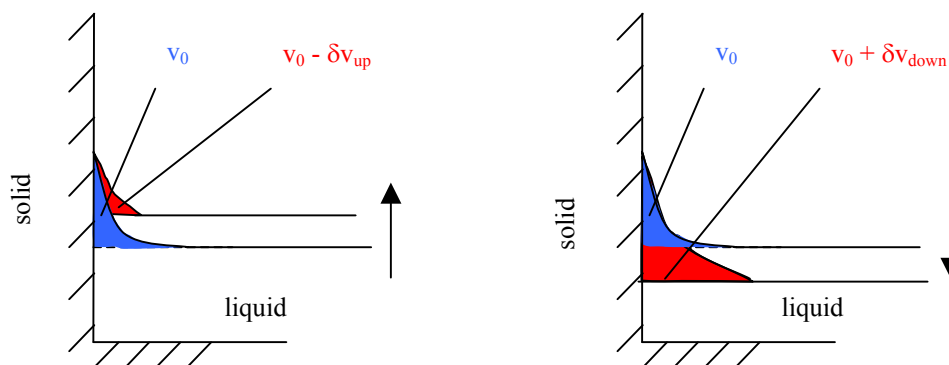


**Figure 7:** Meniscus affect the accuracy of calibration processed by adding or removing a “known” volume in the system (see text). In blue: initial position and shape of the meniscus. In red: position and shape of the meniscus after displacement of the fluids interface (upward on the left, downward on the right).

If one considers the measures operated in differential mode (i.e. signal from one head of the instrument minus signal from the other), this does not affect the final reading since one can show that  $\delta v_{up} \sim \delta v_{down}$  [9]. (This is in principle true as long as the contact line does not move.)

On the other hand, if we consider the measurements in common mode (as it is usually the case in the calibration operated by adding or removing a known volume in the system), this can lead to significant systematic error. Because the estimation of  $\delta v_{up}$  and  $\delta v_{down}$  depends strongly on the physico-chemical properties (i.e. interface tension and contact angles) of the real fluids and solid effectively put together, those systematic errors cannot be accurately calculated based on the theoretical values. In the case of our instrument, an order of magnitude was estimated and the error could have been theoretically as big as 5 to 20% (see [9]). However in practice these errors are much smaller. They do not exceed a few percents, as confirmed by the Earth tides analysis [9]. This can be explained by the fact that at a microscopic level, the real solid surface is not uniform [11]. By consequence the contact angle all along the circumference of the vessel is not the same. Hence, for a given displacement of the interface, the volume of liquid trapped in the meniscus will diminish in some part of the meniscus while it will increase in others. One can hence consider that, on average, the total volume of liquid trapped in the meniscus remains

almost the same. That is why it is recommended to use un-polished vessel walls and fluids with low interfacial tension.

Note also that 1) those theoretical errors are proportional to the inverse of the vessels radius, and 2) surfactants could be used to reduce the interfacial tension and hence reduce these possible errors (as long as the surfactants do not influence the long-term stability of the instrument). Finally, those meniscus errors do not arise in calibrations performed by lifting one vessel with respect to the other.

Remark: that meniscus effect forced us to abandon a former calibration system made of a plunging bar driven by a step motor and a microprocessor. Following a sequence preset by the operator, the bar was automatically immersed more or less deep in the calibration tube installed at the center of the instrument. However, despite its very high repeatability and very low noise (no operator was required in the room), this calibration system provided sensitivity affected by systematic errors of the order of 100%. This was due to the variation of meniscus around the calibration bar, which was of the same order of magnitude as the amplitude of the calibration itself.

## References

- [1] Purcell E., C. Guthmann, P. Lallemand, "Electricité et Magnétisme", 460 pp, Berkeley, Armand Colin, 1973
- [2] National Semiconductor, "LM139/LM239/LM339 A Quad of Independently Functioning Comparators", Application notes 74, 1973
- [3] d'Oreye N., G. Klein, G. Celli, P. Harpes; "WALLACE : From the Intergrated Data Acquisition System to the Database, the Full Remote Control Data Management System for the Walferdange Underground Laboratory", Journ. Geod. Soc. Jpn., vol 47, n°1, pp 47-51, 2001
- [4] d'Oreye N., "The Underground Laboratory of Walferdange: the New Structure", Proc. of 13<sup>th</sup> Int. Symp. On Earth Tides, Roy. Obs. of Belgium, Série Géophys., Brussels, pp 86-97, 1998
- [5] Priestley M.B., "Spectral analysis and time series" (9<sup>th</sup> printing), pp 890, 1996
- [6] Agnew D.C., "Stainmeters and Tiltmeters", Rev. of Geophys., vol 24 N°3, pp 579-624, 1986
- [7] Ogata Katsuhiko, "Modern Control Engineering", 4<sup>th</sup> Edition, Prentice Hall Ed., 2002
- [8] Shepard D., "Dynamic Analysis of a Mercury Tiltmeter", Rep. E-2598, Drapier Lab., Cambridge, Mass., 1971
- [9] d'Oreye N., "Inclinomètre à niveaux hydrostatiques de haute résolution en géophysique", PhD thesis, Univ. Cath. de Louvain-La-Neuve, Belgium, 2003
- [10] Richter B., Wenzel H.-G., "Precise Instrumental Phase Lag Determination by the Step Response Method", Bull. Inf. Marées Terr., N° 111, pp 8032-8052, 1991
- [11] Müller B., M. Riedel, R. Michel, S.M. De Paul, R. Hofer, D. Heger, D. Grützmacher, "Impact of nanometer-scale roughness on contact-angle hysteresis and globulin absorption", Journ. Vac. Sci. Technol., vol. B 19(5), DOI 10.1116/1.1392402, 2001